Phasor Domain Transmission Line Fault Locating with Three Phase Distributed Parameter Modeling

Yu Liu, *Member*, *IEEE*, Zhenyu Tan, *Student Member, IEEE, and* Jiahao Xie, *Student Member, IEEE*

Abstract: Accurate fault locating reduces power outage time and operational costs. In this paper, a novel phasor domain transmission line fault locating algorithm is proposed. Best implementation requires GPS synchronized measurements at both terminals of the line. First, the model of the transmission line with fault is constructed using three phase distributed parameter modeling with neutral conductors and grounding representation. The model is without the assumption that the transmission line is geometrically balanced. Next, the state estimation algorithm is utilized to solve the model of the transmission line with fault, where the fault location is included as a state. Numerical experiments demonstrate that the method has higher accuracy than traditional fault locating methods, independent of fault types, locations and impedances.

Key words: Three Phase Distributed Parameter Modeling, State Estimation (SE), Fault Locating

I INTRODUCTION

ACCURATE transmission line fault locating minimizes the time spent searching for the fault and therefore reduces power outage time and operational costs. Legacy transmission line fault locating techniques are mainly classified into model based methods and measurement based methods.

Model based methods locate the fault based on accurate models of the transmission line of interest. They can be further categorized into phasor-domain model based methods and time-domain model based methods. ***Phasor-domain model based methods*** typically use phasors at the fundamental frequency [1-5]. Single-ended phasor-domain methods utilize phasor measurements from one terminal of the transmission line to locate the fault. However, the main disadvantage of these methods is that they are not accurate with high fault impedances [4]. To solve the above issue, researchers proposed dual-ended phasor-domain methods based on phasor measurements from both terminals of the transmission line, to eliminate the influence of fault impedances [5]. These methods can be further classified into methods that require or do not require GPS synchronized measurements. The main disadvantages of phasor-domain methods are as follows. (a) Most of these methods fail to fully consider the distributed shunt capacitance through the line. Instead, they typically neglect the capacitance or consider them as lumped parameters only at terminals of the line. (b) Most of these methods use sequence line models (sequence lumped parameter models or sequence distributed parameter models), which are based on the assumption that the transmission line is geometrically balanced. (c) The neutral conductors and the grounding of the transmission lines are typically neglected. Besides the phasor domain model based methods, researchers also proposed ***time-domain model based methods*** [6-8]. The main advantage of the time-domain methods over phasor-domain methods is that they do not filter out high frequency components and therefore they are more accurate especially during system transients. Most time-domain model based methods are derived from the Bergeron's method [9], which represent the present voltages and currents at one terminal of the line as functions of the voltages and currents at the other terminal of the line an extremely short period of time (the traveling time of the electromagnetic wave between two terminals of the line) ago. The disadvantages include: (a) the methods need very high sampling rates to ensure accuracy (a proper time resolution is required to accurately express the relationship within this extremely short period of time); (b) most of these methods depend on modal (eg. sequence component) decomposition methods, which also assumes that the transmission line is geometrically balanced; and (c) the neutral conductors and the grounding of the transmission lines are typically neglected. Furthermore, researchers also proposed a time-domain dynamic state estimation based fault locating method [8]. The method utilizes three phase and neutral line models and does not need high sampling rates. However, the method is based on the multi-section cascading π-equivalent model, which is an approximation of the fully distributed line model.

For **measurement based methods**, their accuracy does not depend on accurate modeling of transmission lines. The most widely adopted methods are ***traveling wave based methods*** [10-13]. These methods monitors the arrival time of traveling waves at terminals of the line of interest when a fault occurs inside the line. Single-ended traveling wave based methods [10-11] utilize subsequent wavefront arrival time at the local end and locate the fault by the time differences, including Type A, C, E and F fault locators. Dual-ended methods [12-13] utilize arrival time of the first wavefront at both terminals of the line and locate the fault by the time difference, including Type B and D fault locators. Further, some researchers utilize signal processing techniques such as wavelet transform [14] to accurately detect the wavefront arrival time. The main disadvantages include: (a) the intensity of the traveling wave is related to the inception angle of the fault; (b) the accuracy of the traveling wave based methods highly depends on the sampling rate (eg. 0.93 miles systematic error with Type D fault locator and 100 kilo-samples/second sampling rate).

978-1-5386-7703-2/18/$31.00 ©2018 IEEE

In this paper, a novel phasor domain transmission line fault locating method is proposed. Best implementation requires GPS synchronized measurements at both terminals of the line. The method utilizes three phase distributed parameter modeling with neutral conductors and grounding representation. It accurately models transmission lines without the geometrically balanced assumption. Moreover, the state estimation algorithm [15-17] is adopted to take full advantage of the redundancy inside the fault location problem, to cross check the fault locating results and to improve the fault locating accuracy. The rest of the paper is organized as follows. Section II derives a phasor domain three phase distributed parameter model of the transmission line. Section III provides detail modeling procedure of a transmission line with fault. Section IV demonstrates the state estimation procedure to solve the location of the fault. Section V shows simulation results. Section VI draws a conclusion.

II Phasor Domain Transmission Line Three Phase Distributed Parameter Model

The three phase distributed parameter model of a transmission line can be generated by combining infinite number of infinitesimal sections. In time domain, the model can be expressed via a set of partial differential equations. Afterwards, the following equation can be obtained by substituting time domain waveforms with phasors [18]:

$$\begin{cases} \dfrac{d^2\tilde{\boldsymbol{V}}(y)}{dy^2} = (\boldsymbol{R}_1 + j\omega\boldsymbol{L}_1)(\boldsymbol{G}_1 + j\omega\boldsymbol{C}_1)\tilde{\boldsymbol{V}}(y) \\ \dfrac{d\tilde{\boldsymbol{V}}(y)}{dy} = (\boldsymbol{R}_1 + j\omega\boldsymbol{L}_1)\tilde{\boldsymbol{I}}(y) \\ \textit{Boundary Conditions}:\ \tilde{\boldsymbol{I}}(l)=\tilde{\boldsymbol{I}}_S,\ \tilde{\boldsymbol{I}}(0)=\tilde{\boldsymbol{I}}_R, \tilde{\boldsymbol{V}}(l)=\tilde{\boldsymbol{V}}_S,\ \tilde{\boldsymbol{V}}(0)=\tilde{\boldsymbol{V}}_R \end{cases} \tag{1}$$

where $\tilde{\boldsymbol{I}}(y)$ and $\tilde{\boldsymbol{V}}(y)$ are current and voltage phasor vectors at location y of the transmission line; $\tilde{\boldsymbol{I}}_S$, $\tilde{\boldsymbol{V}}_S$, $\tilde{\boldsymbol{I}}_R$ and $\tilde{\boldsymbol{V}}_R$ are current and voltage phasor vectors at the sending end and the receiving end of the line; $\boldsymbol{R}_1$, $\boldsymbol{L}_1$, $\boldsymbol{G}_1$ and $\boldsymbol{C}_1$ are series resistance, series inductance, shunt conductance and shunt capacitance matrices per unit length.

To solve (1), popular methods adopt modal decomposition methods (such as sequence component transformation, clarke transformation, etc) to transform (1) into a group of scalar equations (corresponding to several independent single phase transmission lines). However, these modal transformations are based on the assumption that (a) the neutral conductors and the grounding of the circuit are negligible, and (b) the transmission lines are geometrically balanced, i.e. the diagonal elements of the parameter matrices $\boldsymbol{R}_1$, $\boldsymbol{L}_1$, $\boldsymbol{G}_1$ and $\boldsymbol{C}_1$ are the same and the off-diagonal elements are the same. These assumptions could potentially generate considerable errors.

To accurately solve (1), the proposed direct method is introduced next. Note that this method does not have the above two assumptions.

The first two rows of (1) can be equivalently expressed as

$$d\tilde{\boldsymbol{W}}(y)\big/dy = \boldsymbol{B}\tilde{\boldsymbol{W}}(y) \tag{2}$$

where $\tilde{\boldsymbol{W}}(y) = \begin{bmatrix} \tilde{\boldsymbol{V}}(y) \\ d\tilde{\boldsymbol{V}}(y)/dy \end{bmatrix}$, $\boldsymbol{B} = \begin{bmatrix} \boldsymbol{0} & \boldsymbol{I}_{n\times n} \\ \boldsymbol{A} & \boldsymbol{0} \end{bmatrix}$, $\boldsymbol{I}_{n\times n}$ is the identity matrix with the dimension of n, and n is the number of conductors of the line, and $\boldsymbol{A} = (\boldsymbol{R}_1 + j\omega\boldsymbol{L}_1)(\boldsymbol{G}_1 + j\omega\boldsymbol{C}_1)$.

The general solution of (2) is,

$$\tilde{\boldsymbol{W}}(y) = e^{y\boldsymbol{B}}\boldsymbol{C} \tag{3}$$

where $\boldsymbol{C}$ is a constant complex vector (to be determined by the boundary conditions), and the matrix exponential function $e^{y\boldsymbol{B}}$ is defined as $\sum_{m=0}^{\infty}(y\boldsymbol{B})^m\big/m!$.

Next, consider the boundary conditions (last row) in (1),

$$\left[\boldsymbol{B}e^{l\boldsymbol{B}}\boldsymbol{C}\right]_{1:n} = \boldsymbol{Z}\tilde{\boldsymbol{I}}_S, \left[\boldsymbol{B}\boldsymbol{C}\right]_{1:n} = \boldsymbol{Z}\tilde{\boldsymbol{I}}_R, \left[e^{l\boldsymbol{B}}\boldsymbol{C}\right]_{1:n} = \tilde{\boldsymbol{V}}_S, \left[\boldsymbol{C}\right]_{1:n} = \tilde{\boldsymbol{V}}_R \tag{4}$$

where the notation $[\bullet]_{a:b}$ means row a to row b of vector $[\bullet]$, and $\boldsymbol{Z} = \boldsymbol{R}_1 + j\omega\boldsymbol{L}_1$.

Define $e^{l\boldsymbol{B}} = [\boldsymbol{M}_{11}, \boldsymbol{M}_{12}; \boldsymbol{M}_{21}, \boldsymbol{M}_{22}]$, where $\boldsymbol{M}_{ij}$ $(i, j = 1, 2)$ is a submatrix of $e^{l\boldsymbol{B}}$ with the dimension of $n \times n$.

From the first two sub-equations in (4), we can express the constant vector $\boldsymbol{C}$ as functions of $\tilde{\boldsymbol{V}}_R$ and $\tilde{\boldsymbol{V}}_S$,

$$\boldsymbol{C} = \left[\tilde{\boldsymbol{V}}_R \quad (\boldsymbol{M}_{12})^{-1}\left(\tilde{\boldsymbol{V}}_S - \boldsymbol{M}_{11}\tilde{\boldsymbol{V}}_R\right)\right]^T \tag{5}$$

Substitute (5) to the last two sub-equations in (4),

$$\begin{cases} (\boldsymbol{M}_{12})^{-1}\left(\tilde{\boldsymbol{V}}_S - \boldsymbol{M}_{11}\tilde{\boldsymbol{V}}_R\right) = \boldsymbol{Z}\tilde{\boldsymbol{I}}_R \\ \boldsymbol{M}_{21}\tilde{\boldsymbol{V}}_R + \boldsymbol{M}_{22}(\boldsymbol{M}_{12})^{-1}\left(\tilde{\boldsymbol{V}}_S - \boldsymbol{M}_{11}\tilde{\boldsymbol{V}}_R\right) = \boldsymbol{Z}\tilde{\boldsymbol{I}}_S \end{cases} \tag{6}$$

From (6), represent $\tilde{\boldsymbol{V}}_S$ and $\tilde{\boldsymbol{I}}_S$ as functions of $\tilde{\boldsymbol{V}}_R$ and $\tilde{\boldsymbol{I}}_R$,

$$\begin{bmatrix} \tilde{\boldsymbol{V}}_S \\ \tilde{\boldsymbol{I}}_S \end{bmatrix} = \begin{bmatrix} \boldsymbol{I}_{n\times n} & \boldsymbol{0} \\ \boldsymbol{0} & \boldsymbol{Z} \end{bmatrix}^{-1} e^{l\boldsymbol{B}} \begin{bmatrix} \boldsymbol{I}_{n\times n} & \boldsymbol{0} \\ \boldsymbol{0} & \boldsymbol{Z} \end{bmatrix} \begin{bmatrix} \tilde{\boldsymbol{V}}_R \\ \tilde{\boldsymbol{I}}_R \end{bmatrix} \tag{7}$$

The above equation (7) is the three phase distributed parameter model of a transmission line. In fact, (7) is a generalization of the modal decomposition based distributed parameter model. **(7) is equivalent to the modal decomposition based model with the following two assumptions: (a) the neutral conductors and the grounding of the line are neglected and (b) for the parameter matrices, the diagonal elements are the same and the off-diagonal elements are the same.** Next, the proof of the above statement is provided.

Proof: Take a three phase transmission line as an example. From the assumption (a) $\tilde{\boldsymbol{I}}_S$, $\tilde{\boldsymbol{V}}_S$, $\tilde{\boldsymbol{I}}_R$ and $\tilde{\boldsymbol{V}}_R$ represent three phase values without neutrals and in this case n = 3.

Here the sequence component transformation is adopted (the proofs are similar for other types of modal decomposition methods). Define sequence component transformation matrix $\boldsymbol{T} = \left[1,1,1; e^{-j120^\circ}, e^{j120^\circ}, 1; e^{j120^\circ}, e^{-j120^\circ}, 1\right]$, we have,

$$\begin{cases} \tilde{\boldsymbol{I}}_S = \boldsymbol{T}\left[\tilde{I}_{S+} \quad \tilde{I}_{S-} \quad \tilde{I}_{S0}\right]^T, \tilde{\boldsymbol{V}}_S = \boldsymbol{T}\left[\tilde{V}_{S+} \quad \tilde{V}_{S-} \quad \tilde{V}_{S0}\right]^T \\ \tilde{\boldsymbol{I}}_R = \boldsymbol{T}\left[\tilde{I}_{R+} \quad \tilde{I}_{R-} \quad \tilde{I}_{R0}\right]^T, \tilde{\boldsymbol{V}}_R = \boldsymbol{T}\left[\tilde{V}_{R+} \quad \tilde{V}_{R-} \quad \tilde{V}_{R0}\right]^T \end{cases} \tag{8}$$

where subscript +, - and 0 correspond to positive, negative and zero sequence values.

From the assumption (b),

$$\begin{cases} \boldsymbol{R}_1 + j\omega\boldsymbol{L}_1 = \boldsymbol{T}diag\left(\left[r_+ + j\omega l_+ \quad r_- + j\omega l_- \quad r_0 + j\omega l_0\right]^T\right)\boldsymbol{T}^{-1} \\ \boldsymbol{G}_1 + j\omega\boldsymbol{C}_1 = \boldsymbol{T}diag\left(\left[g_+ + j\omega c_+ \quad g_- + j\omega c_- \quad g_0 + j\omega c_0\right]^T\right)\boldsymbol{T}^{-1} \end{cases} \tag{9}$$

where $diag([\cdot])$ is the diagonal matrix with column vector $[\cdot]$ as the diagonal elements.

From (9), the matrix $\boldsymbol{B}$ defined in (2) is,

$$\boldsymbol{B} = \begin{bmatrix} \boldsymbol{0} & \boldsymbol{I}_{3\times3} \\ \boldsymbol{A} & \boldsymbol{0} \end{bmatrix} = \begin{bmatrix} \boldsymbol{0} & \boldsymbol{I}_{3\times3} \\ \boldsymbol{T}diag\left(\left[\gamma_+^2 \quad \gamma_-^2 \quad \gamma_0^2\right]^T\right)\boldsymbol{T}^{-1} & \boldsymbol{0} \end{bmatrix} = \boldsymbol{T}_6\boldsymbol{D}\boldsymbol{T}_6^{-1} \tag{10}$$

where $\gamma_i = \sqrt{(r_i + j\omega l_i)(g_i + j\omega c_i)}$ $(i = +, -, 0)$, $\boldsymbol{T}_6 = \begin{bmatrix} \boldsymbol{T} & \boldsymbol{0} \\ \boldsymbol{0} & \boldsymbol{T} \end{bmatrix}$ and

$$\boldsymbol{D} = \begin{bmatrix} \boldsymbol{0} & \boldsymbol{I}_{3\times3} \\ diag\left(\left[\gamma_+^2 \quad \gamma_-^2 \quad \gamma_0^2\right]^T\right) & \boldsymbol{0} \end{bmatrix}.$$

Apply eigenvalue decomposition to matrix $\boldsymbol{D}$,

$$\boldsymbol{D} = \boldsymbol{P}\boldsymbol{\Lambda}\boldsymbol{P}^{-1} \tag{11}$$

where the matrix $\boldsymbol{\Lambda}$ is the diagonal eigenvalue matrix of $\boldsymbol{D}$, and the columns of matrix $\boldsymbol{P}$ are the corresponding eigenvectors,

$$\boldsymbol{\Lambda} = diag\left(\begin{bmatrix} \gamma_+ \\ -\gamma_+ \\ \gamma_- \\ -\gamma_- \\ \gamma_0 \\ -\gamma_0 \end{bmatrix}\right) \quad \boldsymbol{P} = \begin{bmatrix} 1 & 1 & 0 & 0 & 0 & 0 \\ 0 & 0 & 1 & 1 & 0 & 0 \\ 0 & 0 & 0 & 0 & 1 & 1 \\ \gamma_+ & -\gamma_+ & 0 & 0 & 0 & 0 \\ 0 & 0 & \gamma_- & -\gamma_- & 0 & 0 \\ 0 & 0 & 0 & 0 & \gamma_0 & -\gamma_0 \end{bmatrix}$$

Therefore, from equation (10) and (11),

$$\begin{aligned} e^{l\boldsymbol{B}} &= \sum_{m=0}^{\infty}\frac{(l\boldsymbol{B})^m}{m!} = \sum_{m=0}^{\infty}\frac{\left(l\boldsymbol{T}_6\boldsymbol{P}\boldsymbol{\Lambda}\boldsymbol{P}^{-1}\boldsymbol{T}_6^{-1}\right)^m}{m!} = \sum_{m=0}^{\infty}\frac{\boldsymbol{T}_6\boldsymbol{P}(l\boldsymbol{\Lambda})^m\boldsymbol{P}^{-1}\boldsymbol{T}_6^{-1}}{m!} \\ &= \boldsymbol{T}_6\boldsymbol{P}diag\left(\left[e^{l\gamma_+} \quad e^{-l\gamma_+} \quad e^{l\gamma_-} \quad e^{-l\gamma_-} \quad e^{l\gamma_0} \quad e^{-l\gamma_0}\right]^T\right)\boldsymbol{P}^{-1}\boldsymbol{T}_6^{-1} \end{aligned} \tag{12}$$

From equation (9) and (12),

$$\begin{aligned} &\begin{bmatrix} \boldsymbol{I}_{n\times n} & \boldsymbol{0} \\ \boldsymbol{0} & \boldsymbol{Z}_1 \end{bmatrix}^{-1} e^{l\boldsymbol{B}} \begin{bmatrix} \boldsymbol{I}_{n\times n} & \boldsymbol{0} \\ \boldsymbol{0} & \boldsymbol{Z}_1 \end{bmatrix} \\ &= \begin{bmatrix} \boldsymbol{I}_{3\times3} & \boldsymbol{0} \\ \boldsymbol{0} & \boldsymbol{T}diag\left(\begin{bmatrix} Z_+\gamma_+ \\ Z_-\gamma_- \\ Z_0\gamma_0 \end{bmatrix}\right)\boldsymbol{T}^{-1} \end{bmatrix}^{-1} e^{l\boldsymbol{B}} \begin{bmatrix} \boldsymbol{I}_{3\times3} & \boldsymbol{0} \\ \boldsymbol{0} & \boldsymbol{T}diag\left(\begin{bmatrix} Z_+\gamma_+ \\ Z_-\gamma_- \\ Z_0\gamma_0 \end{bmatrix}\right)\boldsymbol{T}^{-1} \end{bmatrix} \\ &= \boldsymbol{T}_6 \begin{bmatrix} diag\left(\begin{bmatrix} \cosh(\gamma_+ l) \\ \cosh(\gamma_- l) \\ \cosh(\gamma_0 l) \end{bmatrix}\right) & diag\left(\begin{bmatrix} Z_+\sinh(\gamma_+ l) \\ Z_-\sinh(\gamma_- l) \\ Z_0\sinh(\gamma_0 l) \end{bmatrix}\right) \\ diag\left(\begin{bmatrix} \sinh(\gamma_+ l)/Z_+ \\ \sinh(\gamma_- l)/Z_- \\ \sinh(\gamma_0 l)/Z_0 \end{bmatrix}\right) & diag\left(\begin{bmatrix} \cosh(\gamma_+ l) \\ \cosh(\gamma_- l) \\ \cosh(\gamma_0 l) \end{bmatrix}\right) \end{bmatrix} \boldsymbol{T}_6^{-1} \end{aligned} \tag{13}$$

Substitute equation (8) and (13) into (7),

$$\begin{cases} \begin{bmatrix} \tilde{V}_{S+} \\ \tilde{I}_{S+} \end{bmatrix} = \begin{bmatrix} \cosh(\gamma_+ l) & Z_+\sinh(\gamma_+ l) \\ \frac{1}{Z_+}\sinh(\gamma_+ l) & \cosh(\gamma_+ l) \end{bmatrix} \begin{bmatrix} \tilde{V}_{R+} \\ \tilde{I}_{R+} \end{bmatrix} \\ \begin{bmatrix} \tilde{V}_{S-} \\ \tilde{I}_{S-} \end{bmatrix} = \begin{bmatrix} \cosh(\gamma_- l) & Z_-\sinh(\gamma_- l) \\ \frac{1}{Z_-}\sinh(\gamma_- l) & \cosh(\gamma_- l) \end{bmatrix} \begin{bmatrix} \tilde{V}_{R-} \\ \tilde{I}_{R-} \end{bmatrix} \\ \begin{bmatrix} \tilde{V}_{S0} \\ \tilde{I}_{S0} \end{bmatrix} = \begin{bmatrix} \cosh(\gamma_0 l) & Z_0\sinh(\gamma_0 l) \\ \frac{1}{Z_0}\sinh(\gamma_0 l) & \cosh(\gamma_0 l) \end{bmatrix} \begin{bmatrix} \tilde{V}_{R0} \\ \tilde{I}_{R0} \end{bmatrix} \end{cases} \tag{14}$$

From the proof above, the proposed model is a generalization of the modal decomposition based distributed parameter model but without the aforementioned two assumptions. Consequently, the proposed model is more accurate.

III Modeling of Transmission Lines with Fault

The transmission line with fault can be accurately modeled with the aforementioned three phase distributed parameter modeling method shown in (7). The mathematical model of the transmission line with fault is a set of complex algebraic equations describing all the physical laws that the transmission line with fault should obey. It has the following format:

$$\begin{cases} \boldsymbol{z}_{vi} = f(\boldsymbol{x}) \\ \boldsymbol{0} = g(\boldsymbol{x}) \end{cases} \tag{15}$$

where $\boldsymbol{z}_{vi}$ is the terminal voltage and current phasor measurement vector of the line with fault, $\boldsymbol{x}$ is the state vector of the system (the location of the fault is one element of $\boldsymbol{x}$). Note that the terminal neutral voltages and currents are introduced as pseudo measurements (zero values but with large error standard deviations) and are included in $\boldsymbol{z}_{vi}$. Also, the second row of (15) corresponds to internal constraints that describe the relationship among elements of the state vector.

In this paper, the modeling of two-terminal lines is presented as an example. Note that similar modeling procedure can be applied to two-terminal, multi-terminal and inhomogeneous transmission lines. The construction process of the model is shown in Figure 1 (a 4-conductor transmission line as an example). It consists of three parts: the line at the left side of the fault, the line at the right side of the fault, and the fault itself. Note that both transmission lines utilize the modeling method in (7). The variables are defined as follows: l_f is the distance between the fault and the left side of the line; l is the total length of the line; $\tilde{\boldsymbol{I}}_1$, $\tilde{\boldsymbol{V}}_1$, $\tilde{\boldsymbol{I}}_2$ and $\tilde{\boldsymbol{V}}_2$ are three phase and neutral current and voltage phasor vectors at both terminals of the line; $\tilde{\boldsymbol{V}}_f$, $\tilde{\boldsymbol{I}}_{f1}$ and $\tilde{\boldsymbol{I}}_{f2}$ are three phase and neutral voltage phasor vector, left side current phasor vector, and right side current phasor vector measured at the location of the fault.

The detail matrices of the model are,

$\boldsymbol{z} = \left[\tilde{\boldsymbol{V}}_1 \quad \tilde{\boldsymbol{I}}_1 \quad \tilde{\boldsymbol{V}}_2 \quad \tilde{\boldsymbol{I}}_2\right]^T$, $\boldsymbol{x} = \left[\tilde{\boldsymbol{V}}_f \quad \tilde{\boldsymbol{I}}_{f1} \quad \tilde{\boldsymbol{I}}_{f2} \quad l_f\right]^T$,

$$f(\boldsymbol{x})=\begin{bmatrix}\begin{bmatrix}\boldsymbol{I}_{4\times4} & \boldsymbol{0}_{4\times4}\\ \boldsymbol{0}_{4\times4} & \boldsymbol{Z}_1\end{bmatrix}^{-1} e^{l_f\boldsymbol{B}}\begin{bmatrix}\boldsymbol{I}_{4\times4} & \boldsymbol{0}_{4\times4}\\ \boldsymbol{0}_{4\times4} & \boldsymbol{Z}_1\end{bmatrix}\begin{bmatrix}\boldsymbol{I}_{4\times4} & \boldsymbol{0}_{4\times4} & \boldsymbol{0}_{4\times4} & \boldsymbol{0}_{4\times1}\\ \boldsymbol{0}_{4\times4} & \boldsymbol{I}_{4\times4} & \boldsymbol{0}_{4\times4} & \boldsymbol{0}_{4\times1}\end{bmatrix}\\ \begin{bmatrix}\boldsymbol{I}_{4\times4} & \boldsymbol{0}_{4\times4}\\ \boldsymbol{0}_{4\times4} & \boldsymbol{Z}_1\end{bmatrix}^{-1} e^{(l-l_f)\boldsymbol{B}}\begin{bmatrix}\boldsymbol{I}_{4\times4} & \boldsymbol{0}_{4\times4}\\ \boldsymbol{0}_{4\times4} & \boldsymbol{Z}_1\end{bmatrix}\begin{bmatrix}\boldsymbol{I}_{4\times4} & \boldsymbol{0}_{4\times4} & \boldsymbol{0}_{4\times4} & \boldsymbol{0}_{4\times1}\\ \boldsymbol{0}_{4\times4} & \boldsymbol{0}_{4\times4} & \boldsymbol{I}_{4\times4} & \boldsymbol{0}_{4\times1}\end{bmatrix}\end{bmatrix}\boldsymbol{x};$$

$$g(\boldsymbol{x})=\begin{bmatrix}\boldsymbol{0}_{n_{fault}\times4} & \boldsymbol{T}_{fault} & \boldsymbol{T}_{fault} & \boldsymbol{0}_{n_{fault}\times1}\end{bmatrix}\boldsymbol{x};$$

where $\boldsymbol{T}_{fault}$ and n_{fault} are defined in Table 1.

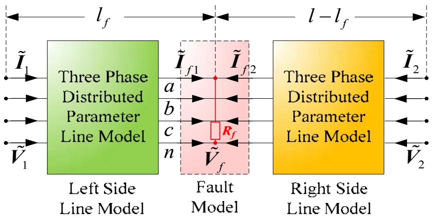

Figure 1. Phasor device model of two-terminal line with fault

Table 1. Values of $\boldsymbol{T}_{fault}$ and n_{fault} for different fault types

Fault Type	*Value of matrix* $\boldsymbol{T}_{fault}$	n_{fault}
A-N	[1 0 0 1; 0 1 0 0; 0 0 1 0]	3
B-N	[1 0 0 0; 0 1 0 1; 0 0 1 0]	3
C-N	[1 0 0 0; 0 1 0 0; 0 0 1 1]	3
A-B	[1 1 0 0; 0 0 1 0; 0 0 0 1]	3
B-C	[1 0 0 0; 0 1 1 0; 0 0 0 1]	3
C-A	[1 0 1 0; 0 1 0 0; 0 0 0 1]	3
AB-N	[1 1 0 1; 0 0 1 0]	2
BC-N	[0 1 1 1; 1 0 0 0]	2
CA-N	[1 0 1 1; 0 1 0 0]	2
3 phase	[1 1 1 0; 0 0 0 1]	2

IV STATE ESTIMATION PROCEDURE

To solve the state vector (including the location of the fault) in equation (15), the state estimation procedure is adopted. The method we use is the unconstraint weighted least square method, where the constraints are treated as virtual measurements (with zero values but with much smaller measurement error standard deviations compared to the actual measurements). Therefore, equation (15) becomes:

$$z=\begin{bmatrix}z_{actual} & \boldsymbol{0}\end{bmatrix}^T=h(\boldsymbol{x}) \tag{16}$$

Note that for two-terminal transmission lines, we have 16 + n_{fault} measurements and 13 states (i.e. 38.5% to 46.2% redundancy) to cross check the fault locating results and improve the fault locating accuracy.

The best estimation of the state vector can be obtained by solving the following optimization problem:

$$\min \quad J=\left(h(\boldsymbol{x})-z\right)^T\boldsymbol{W}\left(h(\boldsymbol{x})-z\right) \tag{17}$$

where $\boldsymbol{W}=diag\left\{\cdots,1/\sigma_i^2,\cdots\right\}$, and σ_i $(i=1,2,\cdots)$ is the error standard deviation of measurement i.

The solution is given with the following Newton's iterative method until convergence:

$$\boldsymbol{x}^{v+1}=\boldsymbol{x}^v-\left(\boldsymbol{H}^T\boldsymbol{W}\boldsymbol{H}\right)^{-1}\boldsymbol{H}^T\boldsymbol{W}\left(h\left(\boldsymbol{x}^v\right)-z\right) \tag{18}$$

where $\boldsymbol{H}=\partial h(\boldsymbol{x})/\partial\boldsymbol{x}\big|_{\boldsymbol{x}=\boldsymbol{x}^v}$.

V SIMULATION RESULTS

The proposed algorithm is validated via a 500 kV, 135.22-mile, two-terminal transmission line of interest (line A1-A2), as shown in Figure 2. The rest of the network is not shown. The tower structure is also shown in Figure 2. Three phase voltage and current measurements are installed at both terminals of the line. Extensive number of events with different fault time, types, locations and impedances has been simulated. The instantaneous measurement data are stored in COMTRADE files for experimentation with the sampling rate of 80 samples per cycle (4.8 kilo-samples per second) according to the IEC61850-9-2LE standard. The phasors of corresponding measurements are afterwards calculated according to the IEEE C37.118 standard.

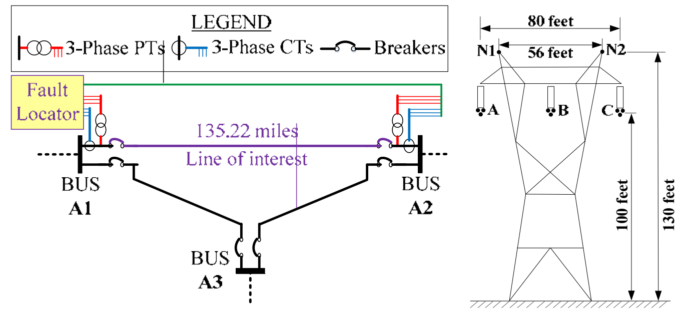

Figure 2. Example test system: two-terminal transmission line

Two legacy fundamental frequency phasor based methods are used for comparison. The two methods are both based on dual-ended three phase voltage and current phasors. The first legacy method (also known as the impedance based method) refers to the IEEE standard [10], which neglects capacitive charging currents through the transmission line and uses sequence line models. The second legacy method uses sequence distributed parameter model of transmission line based on modal (sequence component) decomposition. We compare the proposed method to the above two legacy fault locating schemes via the following test cases. Here we do not consider time-domain model based legacy methods or traveling wave based legacy methods for comparison since their fault locating accuracy cannot be guaranteed with low sampling rates.

Test Case 1: Single Phase to Neutral Faults

A 0.01 ohm phase A to neutral fault occurs at 80 miles from side A1 and at time 1.0 to 1.1 seconds. The fault locating results, including the legacy impedance based method, the legacy modal decomposition based method and the proposed method, are shown in Figure 3. We can observe that the proposed method (79.9660 miles) has higher accuracy compared to legacy impedance based method (81.1237 miles) and legacy modal decomposition based method (80.8011 miles).

To further validate the effectiveness of the proposed method, three groups of phase A to neutral faults at different fault locations, with 0.01 ohm, 1 ohm and 10 ohm fault impedances, are tested. The results are depicted in Figure 4. We can observe that the proposed method is more accurate than both legacy methods.

Test Case 2: High Impedance Faults

Three groups of high impedance phase A to neutral faults at different fault locations, with 100 ohm, 300 ohm and 500 ohm fault impedances, are tested. The results are depicted in Figure 5. We can observe that the proposed method is more accurate than both legacy methods. In this case the maximum absolute error of the proposed method during a 500 ohm high impedance phase A to neutral fault is only around 0.7 miles.

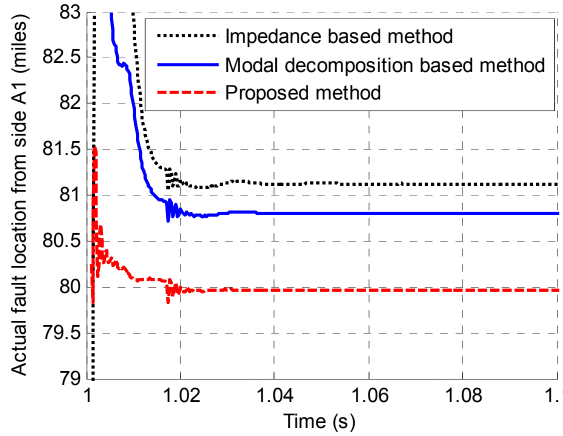

Figure 3. Fault locating results comparison, a 0.01 ohm phase A to neutral fault, 80 miles from side A1

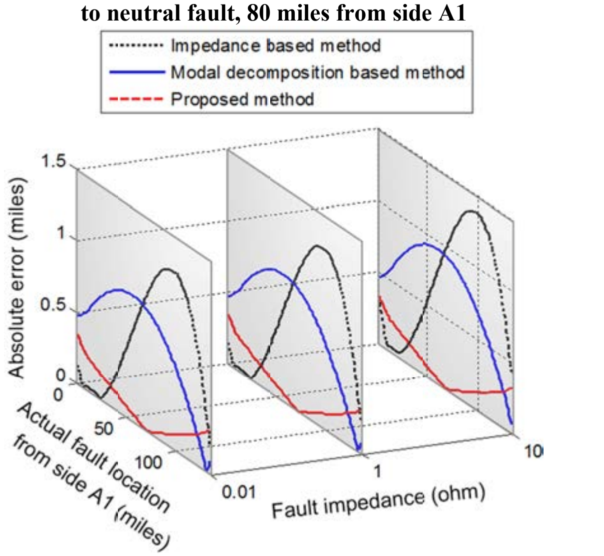

Figure 4. Fault locating results comparison, 0.01 ohm, 1 ohm and 10 ohm phase A to neutral faults, variable fault location

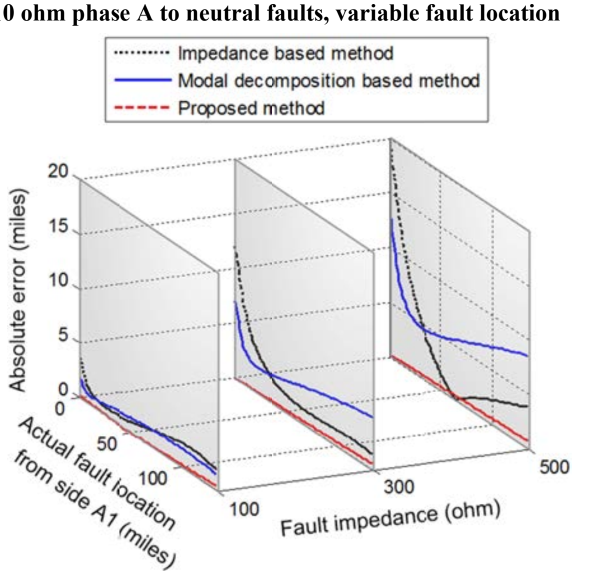

Figure 5. Fault locating results comparison, 100 ohm, 300 ohm and 500 ohm phase A to neutral faults, variable fault location

VI CONCLUSION

A state estimation based phasor domain fault locating algorithm has been presented to accurately determine the fault location in transmission lines. First, the model of the transmission line with fault is built using three phase distributed parameter modeling with neutral conductors and grounding representation. Next, the state estimation algorithm is applied to compute the best estimate of the state (including the location of the fault) of the line with fault. The advantages of the proposed algorithm include: (a) it uses three phase distributed parameter modeling instead of modal (eg. sequence component) decomposition based distributed parameter modeling, and does not assume that the line is geometrically balanced; (b) it considers neutral conductors and grounding representation; (c) it takes full advantage of the redundancy inside the fault locating problem to further improve the accuracy; (d) it demonstrates higher accuracy compared with existing fault locating schemes.

REFERENCES

[1] *SEL-351 Protection System Instruction Manual*, Schweitzer Engineering Laboratories Inc., Pullman, WA, 2015.

[2] GE *D90Plus Line Distance Protection System Instruction Manual*, General Electric Multilin, Markham, Ontario, Canada, 2012.

[3] Siemens *SIPROTEC Line Differential Protection with Distance Protection 7SD5,* Version 4.70, Siemens, Munich, Bavaria, Germany, 2011.

[4] Ha, H., Zhang, B., and Lv, Z., "A novel principle of single-ended fault location technique for EHV transmission lines", *IEEE Trans. Power Del.*, vol.18, no.4, pp. 1147- 1151, Oct. 2003.

[5] Kawady, T., and Stenzel, J., "A practical fault location approach for double circuit transmission lines using single end data," *IEEE Trans. Power Del.*, vol. 18, no. 4, pp. 1166–1173, Oct. 2003.

[6] Song, G., Suonan, J., Xu, Q., *et al*: "Parallel transmission lines fault location algorithm based on differential component net," *IEEE Trans. Power Del.*, 2005, 20, (4), pp. 2396-2406.

[7] Gopalakrishnan, A., Kezunovic, M., McKenna, S. M., *et al*:, "Fault location using the distributed parameter transmission line model," *IEEE Trans. Power Del.*, 2000, 15, (4), pp. 1169-1174.

[8] Liu, Y., Meliopoulos, A. P., Tan, Z., *et al*: "Dynamic State Estimation Based Fault Locating on Transmission Lines," *IET Generation Transmission Distribution*, in press.

[9] Dommel, H. W., "Digital Computer Solution of Electromagnetic Transients in Single-and Multiphase Networks, " *IEEE Trans. Power App. Syst.*, vol. PAS-88, no. 4, pp. 388-399, April 1969.

[10] IEEE Guide for Determining Fault Location on AC Transmission and Distribution Lines, IEEE Standard C37.114, 2014.

[11] Azizi, S., Sanaye-Pasand, M., Abedini, M., *et al.*: 'A traveling wave-based methodology for wide-area fault location in multiterminal DC systems,' *IEEE Trans. Power Del.*, 2014, 29, (6), pp. 2552–2560.

[12] Dewe, M. B., Sankar, S., and Arrillaga, J.: 'The application of satellite time references to HVDC fault location', *IEEE Trans. Power Del.*, 1993, 8, (3), pp. 1295–1302.

[13] Jafarian, P., and Sanaye-Pasand, M.: 'A traveling wave based protection technique using wavelet/PCA analysis', *IEEE Trans. Power Del.*, 2010, 25, (2), pp. 588–599.

[14] Liu, Y., Meliopoulos, A. P., Tai, N., *et al.:* "Protection and Fault Locating Method of Series Compensated Lines by Wavelet Based Energy Traveling Wave", in *IEEE Power Energy Soc (PES). Gen. Meet.*, July. 2017, pp. 1–5.

[15] Zhao, J., Zhang, G., Das, K., Korres, *et al*: "Power system real-time monitoring by using pmu based robust state estimation method," *IEEE Transactions on Smart Grid*, vol. 7, no. 1, pp. 300-309, Jan 2016.

[16] Meliopoulos, A. P., Cokkinides, G. J., Myrda, P., *et al*: 'Dynamic state estimation based protection: status and promise', *IEEE Trans. Power Del.*, 2017, 32, (1), pp. 320-330.

[17] Liu, Y., Meliopoulos, A. P., Fan, R., *et al*: 'Dynamic state estimation based protection on series compensated transmission lines', *IEEE Trans. Power Del.*, 2017, 32, (5), pp 2199-2209.

[18] Meliopoulos, A. P., Power System Grounding and Transients: an Introduction. M. Dekker, 1988.